John W. Weber

Kwong-Chi Wu

Department of Civil and Environmental Engineering
Washington State University
Pullman, Washington 99164

and

Abholhassan Vafai

Shiraz University
Shiraz, Iran

Ultimate Loads for Shallow Funicular Concrete Shells

Abstract

Ten shallow funicular concrete shells (square base, double curvature, and different rises) were loaded to failure with a concentrated central force. Five shells were randomly reinforced with steel wires and the remainder with a wire mesh through the middle surface. All of the shells were 90 x 90 cm in plan form. Strain gages showed a linear relationship between load and strain in the elastic range of the concrete, whereas measured deflections varied nonlinearly with load. In addition, actual deflections were larger than those determined analytically by small deflection theory. These results indicate that large deflection theory, rather than classical small deflection theory, would be more appropriate for theoretical investigations of shallow funicular shells subjected to large concentrated loads. Ultimate loads were not clearly related to type of reinforcement, but were a function of the rise and thickness of the shell; in general, the larger the rise parameter (square of the ratio of rise to thickness), the larger the ultimate load. Failure patterns for shells with both kinds of reinforcement were the same.

Introduction

Because of their light weight, graceful form, and high load resisting capacity, shells of various types are used for many structural purposes. Although shells with potential use in construction have been studied by numerous investigators (Ramaswamy and Chetty 1959, Haas 1961, Ramaswamy 1968, Odello and Allgood 1970, Vafai and Farshad 1976, Farshad 1977, and others), there is a paucity of information on the ultimate strength of funicular shells with different rises. In the case of shells with double curvature (the type discussed herein), classical methods of analysis are complex and unwieldy. The development of the finite element method renders the analysis of such problems tractable, but experimentation is still needed to determine the actual behavior of shells with different reinforcement under various loading conditions; ultimate load and mode of failure are best determined experimentally.

Concrete Mix and Properties

Composition of the concrete mix is shown in Table 1.

Young's modulus, E, was determined by compressive test of standard cylindrical specimens (15.2 x 30.5 cm) cured under the same conditions as the shells. Values of E and other properties of the shells are given in Table 2. A value of 0.10 was used for Poisson's ratio.

TABLE 1. Concrete mix proportions for 1.0 m³.

Mix Component	Amount
Portland cement	1790. kg
Coarse aggregate—traction sand	2130. kg
Fine sand	3690. kg
Water	235. liter
Air entrainment	0.036 kg
*Steel wires (25.4 x 2 mm)	224. kg

*For five randomly reinforced shells; the other five were reinforced with wire mesh (ordinary chicken wire) through the middle surface.

TABLE 2. Properties and failure loads, P_u, of shells.

Shell no.	Reinforcement	Rise, z (cm)	Thickness, d (cm)	$\lambda = \frac{z^2}{d}$	E(x 106) (N/cm2)	P_u (N)	$P_u b^2/Ed^4$
1	RR1	5.61	1.80	9.71	1.655	6,580.	0.835**
2	RR*	5.99	3.00	3.99	1.655	—	—
3	RR	6.30	2.50	6.35	1.379	12,230.	0.502
4	RR	7.01	2.20	10.15	.965	14,230.	1.391
5	RR	7.80	3.80	4.21	1.103	13,340.	0.128
6	WM2	6.91	2.20	9.86	1.517	16,680.	1.038
7	WM	7.39	3.30	5.01	1.517	21,130.	0.259
8	WM	7.80	2.80	7.76	1.517	20,240.	0.480
9	WM*	8.99	2.79	10.36	1.517	—	—
10	WM	9.80	3.30	8.82	1.517	37,360.	0.458

1Random reinforcement (mild steel wires, 2.54 x 0.20 cm).

2Wire mesh (ordinary chicken wire) through middle surface.

*Ultimate loads unrecorded.

**$P_u b^2/Ed^4$ computed with b = 47.0 cm for all shells.

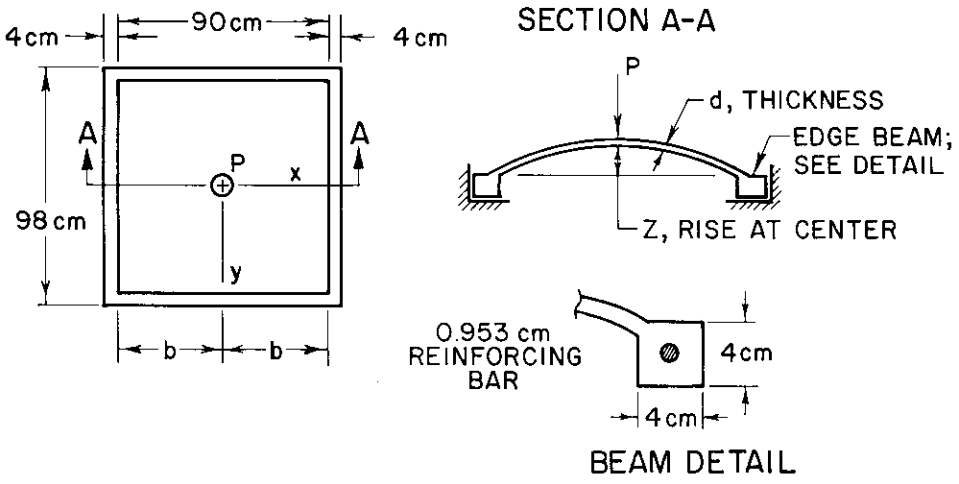

Figure 1. Funicular shell: dimensions, loading, and coordinate system.

Casting of Shells

A form consisting of a square steel frame and canvas was used for casting the shells. The canvas was stretched between the boundaries of the frame and clamped thereto.

When concrete was poured, the resultant sag (and therefore the rise of the shell when in inverted position) was determined by the tension in the canvas; thus, a funiculus was formed. Construction of the frame allowed the casting of four edge beams as integral components of each shell. All shells were moist-cured for 28 days before testing.

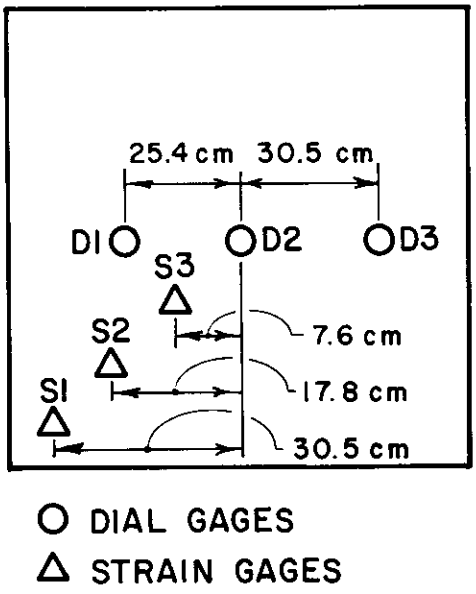

Figure 2. Location of gages (D2 at shell's center).

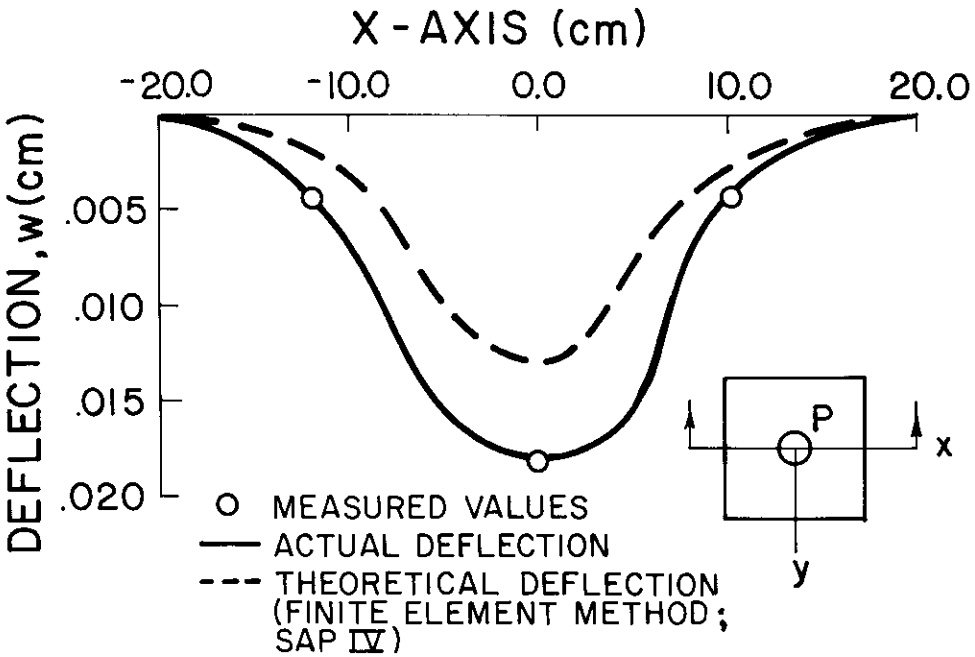

Figure 3. Typical deflection curve (shell no. 4, P = 2020 N).

Instrumentation and Testing

Electrical resistance strain gages (60° strain rosettes) were mounted on the upper and lower surfaces of each shell at intervals along a diagonal, and dial gages were installed to record deflections at several locations along a transverse section through the middle of the shells (Fig. 2). Each shell was loaded in the elastic range, and strains and deflections recorded. After non-destructive testing, all shells were loaded to failure.

Results and Discussion

Measured deflections, as shown in Fig. 3 for a typical case, are large in the region of

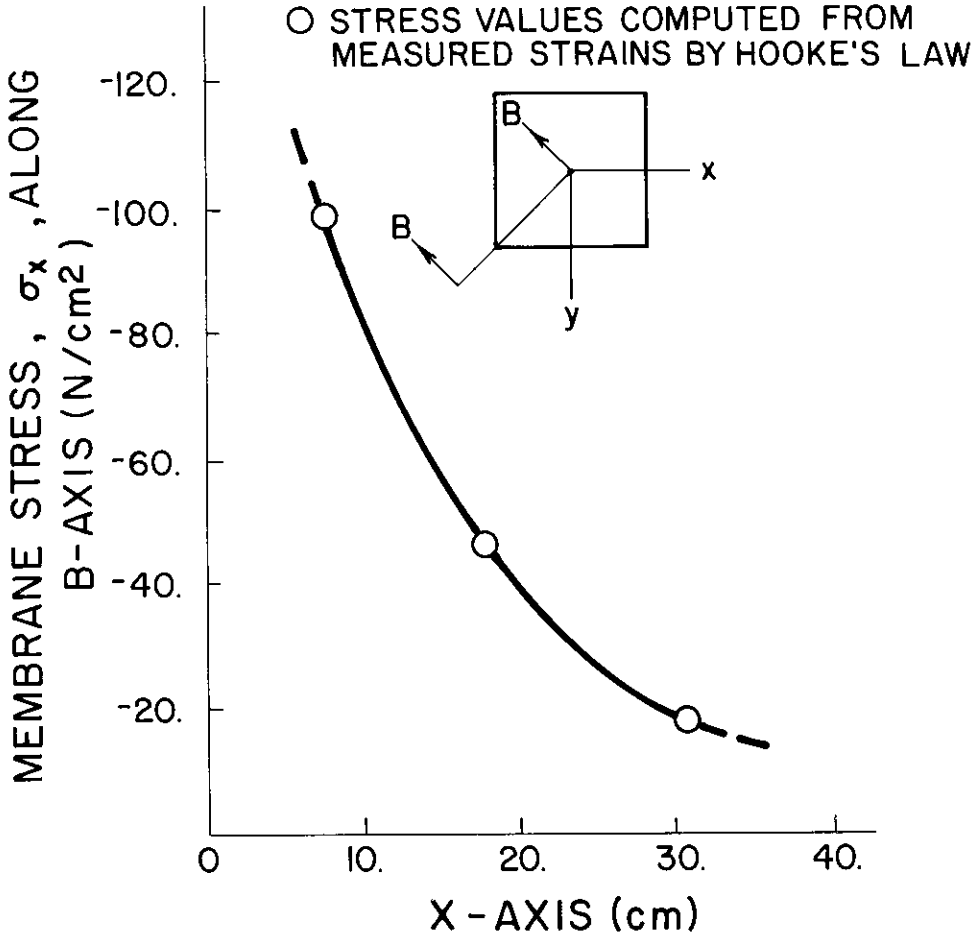

Figure 4. Typical elastic membrane stress curve along B-axis (shell no. 2, P = 4450 N).

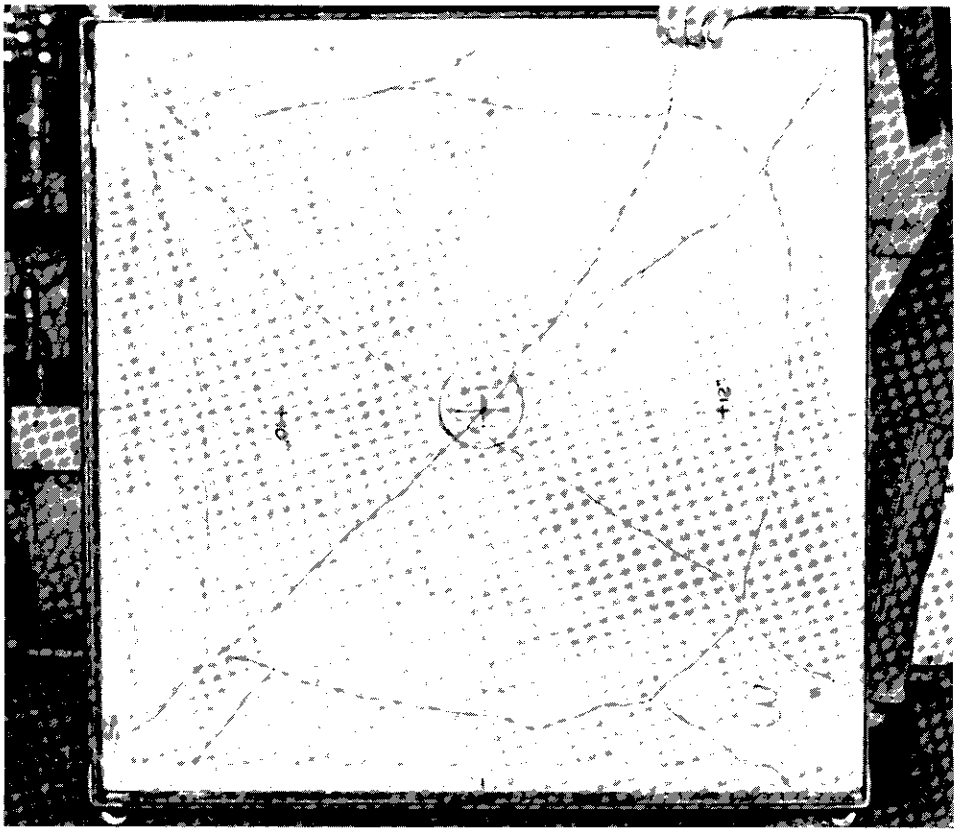

Figure 5. Crack patterns for a typical case (shell no. 3).

the centrally applied force and comparatively small elsewhere. Fig. 3 also shows that measured deflections are greater than those determined analytically by the finite element method (Sap IV thin shell element program with 16 rectangular elements for one quadrant of the shell).

Assuming that bending is localized in the vicinity of the supports and point of load application, membrane theory can be used to approximate the behavior of the shells investigated. A plot (Fig. 4) of the membrane stress distribution (as determined by Hooke's Law from measured strains) for a typical case shows a steep gradient in the vicinity of the load.

At large deflections just before failure, shells with both kinds of reinforcement exhibited the same sequence of crack propagation and crack pattern. Visible cracks first appeared at the center of a shell's outer surface and then propagated to the corners along the diagonals. As the load was increased, apparent zones of tension near and approximately parallel to the supports also cracked (see Fig. 5), forming a mechanism by which the shell eventually failed. Zones of tension in the vicinity of the supports can be attributed to localized bending caused by support reactions.

Although strain measurements indicate a linear variation of strain with load in the elastic range, dimensionless load-deflection plots (Fig. 6) illustrate that load and deflection vary nonlinearly. This behavior and the discrepancy between measured and

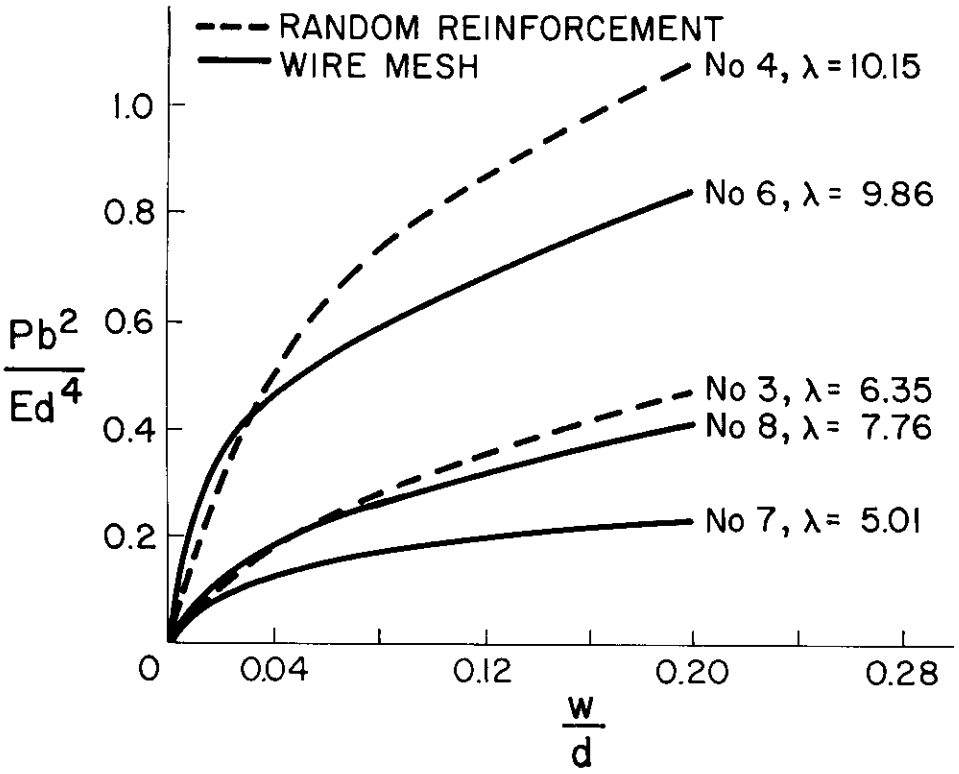

Figure 6. Dimensionless load-center deflection curves for several cases.

theoretical deflections (Fig. 3) suggest that mathematical investigations of shallow funicular shells with large concentrated loads should be based on large deflection theory. Fig. 6 also indicates that the deflection characteristics of a shell vary closely with its rise parameter, λ; type of reinforcement (for the shells tested) appears to have little effect on deflection.

The dimensionless plot in Fig. 7 shows the variation of the failure load, P_u, with λ. In general, P_u increases with large values of λ. For the shells tested, Fig. 7 shows that the load resisting capacity of a shell, regardless of the kind of reinforcement, is primarily a function of its rise and thickness. By Fig. 7, the relationship between P_u and λ can be approximated by the equation ($2 \leq \lambda \leq 11$)

$$\frac{P_u b^2}{Ed^4} = 0.0603 e^{0.2197\lambda}$$

Extrapolation of the dimensionless results in Fig. 7 to shallow funicular shells different in size from those discussed in this study requires caution, since other modes of failure are possible. For example, Odello and Allgood (1970), who tested funicular shells 10.67 x 12.20 m in plan with a 5.08 cm thickness and a 76.2 cm rise ($\lambda = 225$), found that uniformly loaded shells failed by buckling and that shells subjected to concentrated loads failed by punch shear. Additional experimental work on shells of sizes transitional between those discussed herein and those considered by Odello and All-

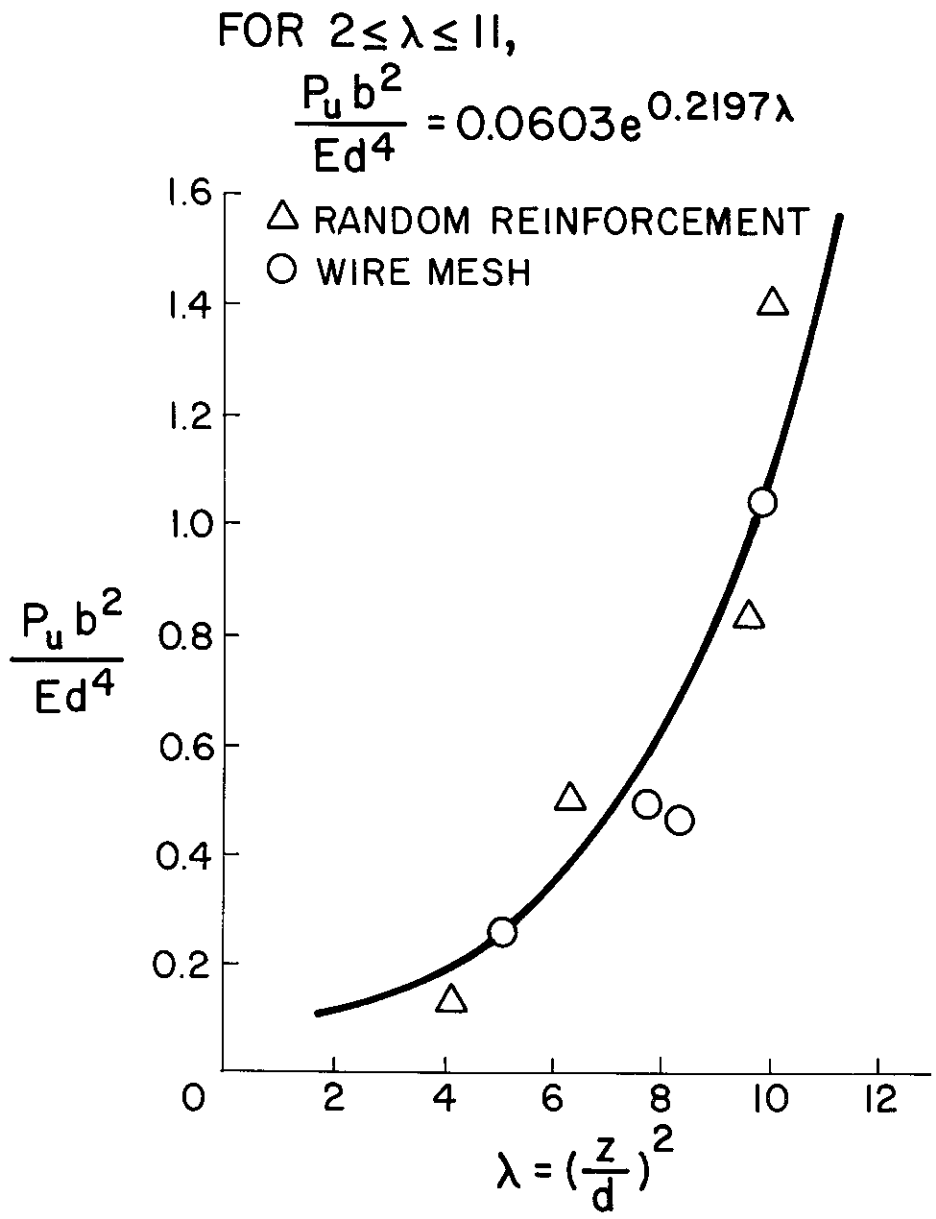

Figure 7. Variation of ultimate load parameter, $P_u b^2/Ed^4$, with rise parameter, λ.

good should be undertaken to further the understanding of failure loads for funicular shells.

Acknowledgments

The writers thank R. J. Hoyle, Washington State University, for his laboratory assistance.

Literature Cited

Farshad, M. 1976. Shell Structures. Shiraz University Press, No. 84. Shiraz, Iran.
Haas, A. M., and A. L. Bouma. 1961. Shell research. Proceedings of the Symposium on Shell Research, Delft. North Holland Publishing Co., Amsterdam.
Odello, R. J., and M. R. Allgood. 1970. Concrete funicular shells for floors and roofs. Technical Report R-693, YF 38.534.001.01.003. Naval Civil Engineering Laboratory, Port Hueneme, Calif.
Ramaswamy, G. S. 1968. Design and Construction of Concrete Shell Roofs. McGraw-Hill, N.Y.
———, and S. M. K. Chetty. 1959. A new form of double-curved shell for roofs and floors. The International Association for Shell Structures. Bulletin 1. a-4. Internation Colloquium on Construction Processes of Shell Structures, Madrid, Spain.
Vafai, A., and M. Farshad. 1976. Investigation of pointed domes—II. Experiment. Building and Environment 11:87-90.

Received December 26, 1982
Accepted for publication April 19, 1983